Plant Soil (2026) 523:479–497
https://doi.org/10.1007/s11104-026-08632-2

RESEARCH ARTICLE

A minimally destructive method for 2-dimensional soil and root mapping in row crops

M. D. McDaniel · C. R. Dutter · M. Eness · A. Cecil · B. A. Miller · M. Modestou

Received: 29 October 2025 / Accepted: 1 May 2026 / Published online: 25 May 2026

Abstract
Background&Aims Monitoring belowground soil–plant interactions in the field remains challenging and limits our ability to inform and improve agricultural management. Our primary objective was to develop two-dimensional (2D) maps of soil and root properties using a minimally destructive, paired soil-root co-sampling strategy in a long-term, small-plot experiment. Our secondary objective was to test two hypotheses: H1) soil and root properties mirror one another across the crop row, and H2) strip-tillage and in-row fertilization will cause localized effects relative to the interrow.
Methods We collected 90 soil and 90 root samples from three 6.86 × 6.10 m plots using a staggered, paired sampling design. Samples were reconstructed into 2D grids centered on the Zea mays (maize) row (76 × 30 cm). We measured bulk density (ρ_b), gravimetric water content (θ_g), pH, electrical conductivity (EC), ammonium (NH_4^+-N), nitrate (NO_3^--N), salt-extractable organic N, root biomass, root length density (RLD), and mean root diameter (MRD) to evaluate H1 and H2.
Results 2D maps of soil and root properties were broadly consistent across the three plots, though optimal interpolation models varied. H1 was partially supported: 6 of 11 variables were correlated across sides of the row. Row management influenced 8 of 11 variables, supporting H2. The strongest in-row effects occurred for NH_4^+-N > root biomass, RLD > NO_3^--N > EC > ρ_b.
Conclusion This minimally destructive co-sampling and mapping approach enables simultaneous characterization of soil and root distributions at the plant scale (0.05–1 m). We recommend its application in other agroecosystems to evaluate row-crop management practices.

Keywords Choropleth map · Fertilizer banding · Interpolation · Rhizosphere · Soil-root interactions

Responsible Editor: Xiaolin Yang.

Supplementary Information The online version contains supplementary material available at https://doi.org/10.1007/s11104-026-08632-2.

M. D. McDaniel (✉) · C. R. Dutter · M. Eness · A. Cecil · B. A. Miller · M. Modestou
Department of Agronomy, Iowa State University, Ames, IA 50011, U.S.A.
e-mail: marsh@iastate.edu

Introduction

Knowing where things are, and why, is essential to rational decision making.

– Jack Dangermond[1]

Our struggle to measure and map belowground interactions between plant roots and soils limits the agriculture sciences. While technologies like rhizoboxes and plant root phenotyping scanners have advanced our ability to measure crop root dynamics in greenhouse or growth chamber settings, measuring crop roots and the surrounding soil in situ remains a formidable challenge (Böhm 2012; Freschet, et al. 2021a, 2021b; Taylor 1986). Mini-rhizotrons and root exclusion cores have allowed some repeated measures of root growth, but these methods have their own limitations, such as difficulty extrapolating to field-scale and excessive labor required (Freschet, et al. 2021a, 2021b). Furthermore, they do not allow researchers to collect soil and roots near one another at the plant scale (cm to 1 m).

The challenge of measuring soil and root properties at this scale is often compounded by the destructive nature of sampling roots and soils in the field, i.e., most commonly done with the "shovel-and-shake" method (Wasson et al. 2020; Wollum 1994). The shovel-and-shake method, which relies on using a shovel to pry a crop from the row, allows one to separate soil into interrow, row, and "rhizosphere," if rhizosphere is defined as soil closely associated with or bound to plant roots. Researchers using this shovel-and-shake method can isolate soils increasingly under the influence of crop roots from interrow < row < "rhizosphere" (Finzi et al. 2015; Gomes et al. 2003; Wollum 1994).

Better exploring where roots and soil resources overlap, and at the plant scale, is key to better understanding and managing row crop agroecosystems. Especially agroecosystems under precision management, which are becoming the norm in developed regions with access to geospatial technologies. As geospatial technologies achieve finer resolutions at field scales, so do precision practices like seed planting, strip tillage, and targeted fertilizer placement at the plant scale. Modern equipment for these now common agricultural practices is accurate at sub-10—cm-scale precision (Gao et al. 2023; Nardon & Botta 2022; Wang et al. 2023).

One approach to better understanding agroecosystems under this precision management is to vertically map soil and root properties at the plant-scale (or in the z-dimension). This would provide a cross-section visual representation of soil–plant root systems within a crop row. Precise management practices – like strip tillage or banded fertilizer – will undoubtedly alter the spatial distribution of roots, bio-available nutrients, active pH, low-molecular-mass organic compounds, microbial biomass, and other properties of interests. And mapping how precision management affects soils or crops at this scale can help improve management to enhance overall agroecosystem functioning. For example, sampling and mapping soil-root systems in this two-dimensional (2D) space has provided insights into the management effects of practices like intercropping (Liu et al. 2020), irrigation (Nightingale et al. 1986), and tillage practices (Sun et al. 2023).

Researchers have been plotting relationships between soil or roots in this vertical 2D space across a crop row for several decades (Fig. 1); but the idea originated from the more qualitative soil profile descriptions and drawings commonplace in soil pedology. However, digital soil morphometrics has leveraged modern technologies to expand the capabilities of soil profile analysis, especially in terms of quantitative measurements at finer spatial resolutions (Hartemink and Minasny, 2014). In other words, new precision technologies and interests in finer-scale soil management have moved from more qualitative soil profile descriptions to more quantitative, finer-scale applications. And this has been further enabled by technological advances in data visualization and digital mapping. In the same way that fields can be mapped using x-, y- dimensions, i.e., latitudinal and longitudinal coordinates, researchers can also map soil and roots in horizontal (x- or y-axes) and vertical (z-axis) distances. However, studies mapping soil–plant interactions have been limited by sampling methods, but maybe even more so by accurately interpolating between observation points.

From a measurement perspective, one advantage of row crop systems is their uniform management. Modern machinery and technology facilitate evenly applied chemicals and uniform plant populations, in unprecedented precision. This systematic, uniform way to manage crop rows has presumably created a uniform potential for plant growth, which presumably

[1] co-founder and president of Environmental Systems Research Institute. ESRI are the makers of ArcGIS (Geographic Information Systems) software.

led to root growth patterns that can be generalized for a plot or even a given field. However, this underlying assumption does not consider the spatial variability of soils in all three dimensions.

We leveraged a long-term experiment with strip-tilled plots of continuous *Zea mays* (maize) to produce 2D soil-root maps and then tested two hypotheses. This required a novel, strategic, and minimally destructive sampling campaign to form a representative vertical grid of three individual plots from this experiment. We used a paired and staggered sampling approach to form a 76 × 30 cm (width × depth) grid centering on the maize row with n = 90 for each plot (Figs. 2, S1). Then we reconstructed the distribution

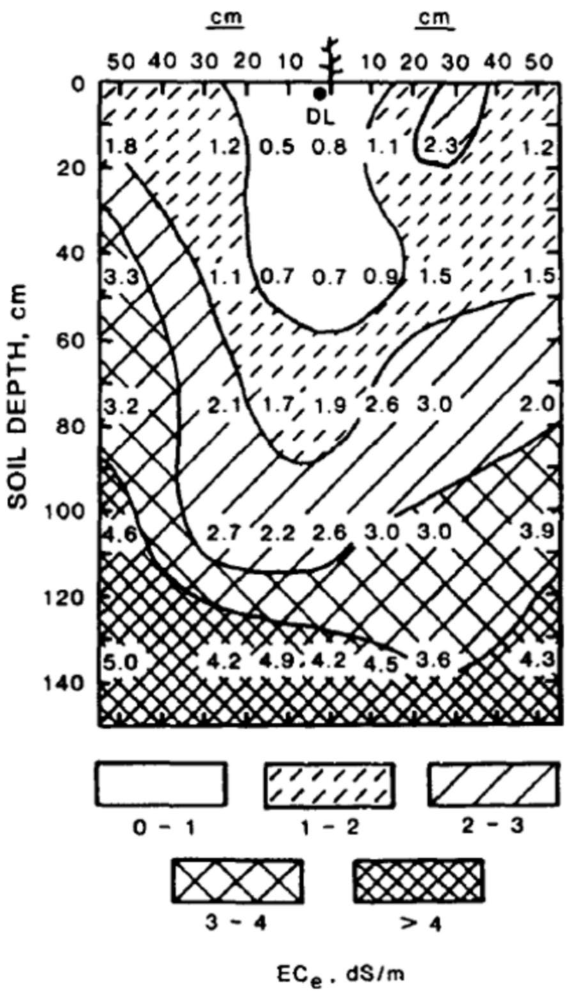

Fig. 1 Isopleth maps of soil electrical conductivity (EC_e) measured within 50 cm distances from either side of cotton row, and down to 140 cm. DL shows the drip-line irrigation. Original figure from Nightingale et al. (1986)

of soil and root properties within each of the replicated plots and tested various spatial interpolation models for each plot. Our objectives were three-fold:

1) Quantitatively identify the best interpolation method to map soil and roots properties at the plant scale when maize is at V6 growth stage;
2) test a hypothesis of spatial symmetry for 11 soil and root properties (H1, Fig. 1b), assuming the axis of symmetry is where the maize is planted; and
3) determine the "row effect" on soil and root properties (H2, Fig. 1c). The "row effect" is a combination of strip tillage, row fertilizer placement, and concentrated maize root biomass. We chose to compare the "row effect" only at the 0—15 cm depth because of the tendency for soil fertility sampling to take place at this depth.

There are other similar studies that have created 2D maps of soil and/or roots at the plant scale (Table 1). Few, however, have paired both root and soil samples to make connections between the two (notable recent exceptions: Liu et al. 2020; Sun et al. 2023). To our knowledge, no study has sampled as intensively at this plant scale (395 samples m^{-2}, Table 1); and tested multiple spatial interpolation models that are normally used at the field scale. This combination of approaches is the first of its kind, but the technique could be applied to any plot-level work where researchers are interested in the paired distribution of root and soil properties.

Materials and Methods

Site characteristics & experimental design

Soil samples were collected from a long-term experiment established in 2018 at the Sorensen Farm near Boone, IA (42.009453, −93.741142). This long-term experimental design was a randomized complete block design with several treatments, including perennial groundcover or living mulch treatments, and a control continuous maize with four replications. The plot size was 6.86 × 6.10 m to accommodate an eight-row planter and strip-tiller (0.76 m row spacing). The replications (or blocks) were separated by a 6—m alleyway seeded with tall fescue and mowed regularly.

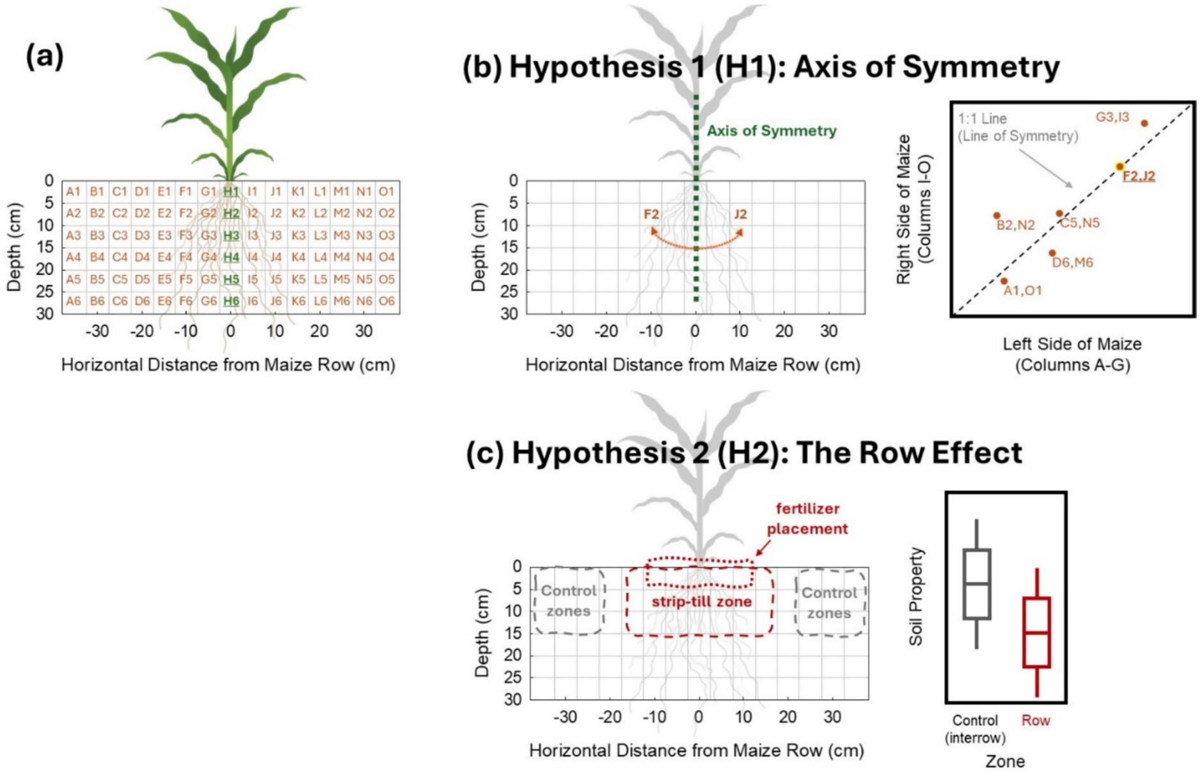

Fig. 2 **a)** Cross-section of maize plant with 2-dimensional, vertical & horizontal, sampling grid at scale when maize is at V6 growth stage. Soil and root sampling grid created from paired, staggered soil and root sampling. Each cell in the grid is labeled by columns (letters) and rows (numbers). **(b)** Hypothesis 1 (H1), Axis of Symmetry or AOS): soil and root properties should be correlated with the mirror soil sample (excluding the AOS). For example, soil/root sample F2 should correlate with J2. **(c)** Hypothesis 2 (H2, The Row Effect): showing strip tillage and fertilizer placement in row [and paired control zones (interrow)] with a hypothesized outcome of the"row effect." Maize drawing credit: ©Olivia Pavlak 2024

Within this block design, three plots from the control continuous maize treatment were sampled for this study. These are located in a toposequence that, within a relief of 1 m, is mapped as grading from a naturally poorly drained soil to a well-drained soil. The field is tile drained, but the plot in the poorly drained soil is at the base of the slope and is mapped as a Webster clay loam (Fine-loamy, mixed, superactive, mesic Typic Endoaquolls, 0—2% slope) (Soil Survey Staff 2024). The plot in the intermediate position is in a Nicollet loam map unit (Fine-loamy, mixed, superactive, mesic Aquic Hapludolls, 1—3% slope), and the uppermost plot is located in a Clarion loam map unit (Fine-loamy, mixed, superactive, mesic Typic Hapludolls, 2—6% slope). The climate at the site is classified as Dfa according to Köppen-Geiger climate classification, with a 50-year mean annual temperature at the sampling location of 9.7 ℃, and a mean annual precipitation of 945 mm (Mesonet 2024).

The crop rows are disk-tilled annually between 1 April to 15 May with a Unverth 330 Ripper Stripper, which disrupts soils to a 15 cm depth and 38 cm width centered on the maize row (Fig. 1b). In 2023, the soil was tilled on 12 April. Then, on 3 May, maize (DeKalb DK57—75) was planted at 6 cm depth. Farm equipment passes are minimized where possible, and both human and machine traffic is confined to interrows.

All fertilizer was added in surface bands about 10 cm to the left and right of the crop row center (Fig. 1b). Solid nitrogen (N) fertilizer is added as urea at 168 kg N ha^{-1} between 24 April and 4 May.

Table 1 Select studies that have created 2D maps of soil and/or root parameters using minimally destructive soil coring in an agricultural context

First author last name	Year	Horizontal Distance (cm)	Vertical Distance or Depth (cm)	Number of samples (n)	Sampling Density (n m^{-2})*	Soil Parameters†	Root Parameters‡	Context
Nightingale	1986	51	150	30	39	EC		Irrigation management
Robbins & Voss	1991	75	25	45	240	STK, STP		Tillage practices (esp. on P stratification)
Hollanda	1998	82	25	55	259	STK, STP		Tillage practices (esp. on P stratification)
Li	2006	50	60	30	100		RLD	Intercropping
Gao	2010	70	90	70	111		RLD, absence/presence crop,	Intercropping
Xia	2013	80	100	80	100		RLD	Intercropping and P application
Steusloff	2019	76	61	35	75	pH, NH_4^+, NO_3^-		Effect of claypan and fertilizer band
Liu	2020	70	100	80	114	NH_4^+, NO_3^-	RLD	Intercropping
Bi	2022	100	50	50	100	NH_4^+, NO_3^-		Fertigation
Oliveira	2022	75	30	35	156	total P, SOC, organic P, M3P		Phosphorus management
Sun	2023	70	50	25	71	ρ_b, porosity	root biomass, RLD, surface area	Tillage practices
Dong	2024	96	60	64	111		RLD, surface area	Intercropping
Dou	2024	30	40	8	67	urease, PHOSase, INVase		Irrigation dripline
Liu	2024	40	60	24	133	θ_g, NO_3^--N	RLD	Fertigation
This study	**2025**	**76**	**30**	**90**	**395**	**ρ_b, θ_g, pH, EC, NH_4^+, NO_3^-, SEON, MBN**	**root biomass, RLD, MRD**	**Strip-tillage and fertilizer band**

* per plot sampling density

† ρ_b = bulk density, EC = eleoctrical conductivity, INVase = invertase, θ_g = gravimetric water content, NH_4^+ = ammonium, NO_3^- = nitrate, MBN = microbial biomass N, PHOSase = acid phosphtase, SEON = salt-extractable organic N, STK = soil test potassium, STP = soil test phosphorus (e.g., mehlich III)

‡ RLD = root length density, MRD = mean root diameter

Phosphorus, potassium, and sulfur are added as diammonium phosphate at 112 kg P ha^{-1}, potash at 123 kg K ha^{-1}, and sulfur as encapsulated urea at 13.3 kg S ha^{-1} typically between 24 April and 17 May (also adds additional 39 kg N ha^{-1}).

Soil & root sampling to convert a 3D plot to a 2D psuedogrid

Soil cores were collected on 15 and 16 June 2023 when maize was at V6 with a 3.2 cm diameter probe (JMC; Newton, IA). Six 30—cm deep cores were precisely collected at 15 distances, spaced at 5 cm, from the center of the maize row using wooden boards with holes drilled for a soil probe (board dimensions = 2 × 10 × 152 cm; Figure S1). Each 30—cm deep core collected at a given horizontal position was then subdivided into six depths in the field (0—5, 5—10, 10—15, 15—20, 20—25, and 25—30 cm depths). Then, the six corresponding sub-samples at each horizontal position and depth were composited for a total of 90 samples for soil and roots at each plot. These 90 samples represented a 2-dimensional psuedogrid of soil and roots that is 75 cm wide and 30 cm deep at 5—cm increments (Fig. 1a). This systematic sampling was repeated for three plots, for a n = 3 replicated plots, each with a grid of 90 samples comprised of soil and roots. The soil and root samples were stored in a cooler until reaching the laboratory. Samples were stored there for two to three weeks at 4 °C in a refrigerated room, after which the root and soil samples proceeded on two different analysis paths (Fig. 3).

On these isolated soils and roots – collected from when maize is at rapid growth and greatest N uptake – we selected three root characteristics and eight soil properties related to either root morphology (or abundance), plant-available N, or just general soil fertility. The three root properties are: root biomass, root length density (RLD), and mean root diameter (MRD). The

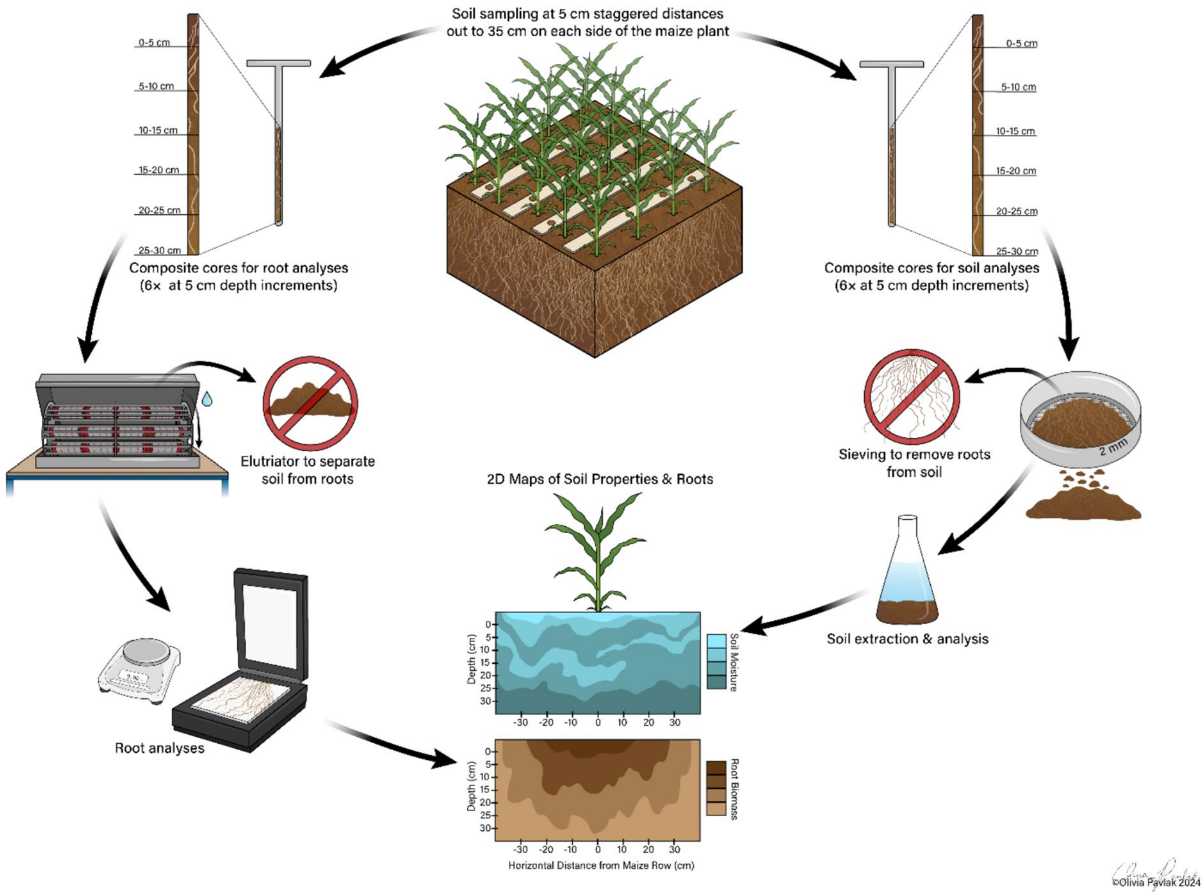

Fig. 3 Paired, staggered soil and root sampling scheme to create 2-dimensional, contour maps of root and soil properties within a rowcrop system. *Left half*: shows processing of root samples. *Right half*: shows processing of soil samples. See Figure S1 for more on paired, staggered soil and root sampling. Illustration credit: ©Olivia Pavlak 2024

eight soil properties are: bulk density (ρb), gravimetric water content (θ_g), pH, electrical conductivity (EC), ammonium N (NH_4^+-N), nitrate N (NO_3^--N), microbial biomass N (MBN), salt-extractable organic N (SEON). We focus on soil N pools is because there is a soil N test, the late spring nitrate test, that is used by Midwest US farmers for maize N recommendations are taken at this V6 growth stage (Blackmer et al. 1989).

Root analyses

Root samples were initially cleaned of soil using a custom-made rotary elutriator (sensu Elutriator-48X; R-Tech Industries Ltd.; Homewood, MB, Canada; Dietzel et al. 2017). Root samples were washed in the elutriator for 1 h. To remove further soil from the roots, samples were placed in 0.53 µm sieves washed with water, allowing lighter root mass to float to the surface, with the remaining mineral soil and associated organic matter sinking to the bottom or washing through the sieve. The separated, wet roots were stored at 5 °C to prevent decomposition for a maximum of three weeks before being scanned for root morphology measurements.

Before scanning, the roots were suspended in DI water in a 30×42×5 cm (W×L×H) clear acrylic box tray for dispersion. The roots in water were then scanned on an Epson Expression (Epson; Suwa, Japan) at 640 dpi and grayscale. We analyzed the images using RhizoVision Explorer (Seethepalli et al. 2020). Any non-root objects remaining in scans were ignored using RhizoVision's native functions, although any clearly foreign object was removed before scanning. We focused here on the RhizoVision outputs of total root length within each soil core, to calculate root length density (RLD) in mm of root per cm^3 of soil (mm cm^{-3}), and mean root diameter (MRD) in mm. Finally, after scanning, root samples were dried at 70 °C for 72 h. Following drying, each sample was weighed for total mass.

Soil analyses

Soil samples were sieved (<2 mm) and dried at 105 °C for 24 h to determine θ_g. The total mass of the dry soil and volume of eight cores were used to calculate ρ_b in grams of dry soil per cubic centimeter (g cm^{-3}). On these air-dried soil samples, we also measured soil pH and EC in a 1:1 (w:w) soil water slurry with a HQ440D combo meter (Hach, Loveland, CO, USA).

On fresh soil, we extracted ammonium and nitrate using 25 ml of 0.5 M K_2SO_4, and extracts were measured for NH_4^+-N and NO_3^--N using a Synergy HTX Multi-Mode Microplate Reader (BioTek Instruments, Winooski, VT, USA) with Gen5 software. Ammonium-N was measured using salicylate and ammonia cyanurate reagent packets absorbance at 595 nm wavelength (Sinsabaugh et al. 2000); and NO_3^--N was measured using single-reagent method, azo dye using Griese reagent, and read at an absorbance at 540 nm wavelength (Doane & Horwáth 2003). Nitrate in these samples, as with many agricultural samples, was assumed to be negligible.

We also analyzed fresh soil for N in MBN and SEON. We used the chloroform fumigation-extraction method (Brookes et al. 1985; Vance et al. 1987) but modified according to (Dutter et al. 2024). Both MBN and SEON extracts were run on a TOC/N-L (Shimadzu; Kyoto, Japan). No extraction coefficients were used.

Data handling & statistical analyses

First, data were filtered for outliers. We deemed any value beyond two standard deviations within an individual plot an outlier (n = 90). With outliers and missing samples, analytes range from missing no values to missing up to 23 (out of 270 values). Then data were checked for normality and heterogeneity of variances using *ggResidpanel* (version 0.3.0; Goode & Rey 2019) in the statistical software R (v. 4.3.1; R Core Team 2023).

To test H1 (Axis of Symmetry), we regressed the left coordinate (horizontal positions A through G) with the mirrored right values (horizontal positions I through O, Fig. 2a), respective of the crop row. Then we used a multitier approach to evaluate "mirrroredness." First, was to test a full main and interactive linear mixed effect model (LMM), using *lmer* function in lme4 (Bates et al. 2014), to correct for autocorrelation and any interactions with depth. Second, we found no evidence for strong interactions, so we fit a reduced LMM that accounted for main effects of the mirrored correlation and depth separately (Eq. 1).

$$X_R = \beta_0 + X_L + Depth + (1 + Depth|Random) \tag{1}$$

where X_R and X_L are the variables across depths on their respective right and left sides of the row crop. β_0 is the LMM intercept. *Depth* is the within-depth contributions, or main effect, component of the LMM. We allowed both random intercepts and random slopes. *Depth* was thus fixed, but in the *Random* term includes horizontal distance nested within block.

Second, with this reduced LMM, we used a suite of complimentary tests that provide evidence for H1 (or "mirroredness") based on two criteria: i) strength of the correlation between left and right variables (Nakagawa's pseudo-R^2; Nakagawa & Schielzeth 2013), and ii) similarity with a slope = 1 (Confidence Interval Test and Null Hypothesis H_0: Slope = 1). In addition, we also calculated Lin's Concordance Correlation Coefficient that covers both criteria i) and ii) using Eq. 2:

$$\rho_c = \frac{2\sigma_{xy}}{\sigma_x^2 + \sigma_y^2 + \left(\mu_x - \mu_y\right)^2} \tag{2}$$

where μ_x and μ_y are the means of the two variables, σ_x^2 and σ_y^2 are their variances, and σ_{xy} is the covariance between the two variables (Lawrence & Lin 1989). In our case, the value likely ranges from 0 to 1, where a value closer to 1 reflects high positive agreement between the left and right sides of the crop row.

To test H2, we used a linear mixed-effect model. The NH_4^+-N, root biomass, and RLD data were log transformed, and the NO_3^--N, SEON, and MBN data were square root transformed. The fixed effects were tillage treatment (No-till vs. Strip till) and replication (a 3-level categorical variable). The random effects were horizontal positions (a 13-level categorical variable) and sample depth within each horizontal position (six per horizontal position) to account for the potential dependence in the same horizontal position. The model equation is given by Eq. 3:

$$y = treatment + block + \left(\frac{1}{x \bullet position}\right) + \left(\frac{z \bullet position}{x \bullet position}\right) \tag{3}$$

Boxplot and regression data were visualized using SigmaPlot v15 (Grafiti LLC; Palo Alto, CA).

Plant-scale profile mapping statistics

Composite soil samples, although collected in three dimensions within a plot, were collapsed and treated as if collected at single locations at the center of their volumetric position. These values were then plotted on a 2-D Cartesian coordinate system to represent each plot. These points were interpolated using three methods to produce a continuous geographic field: inverse distance weighting (IDW), cubic spline, and ordinary kriging. To implement IDW interpolation, we applied Eq. 4 using Python.

$$\hat{y} = \frac{\sum_i^n w_i y_i}{\sum_i^n w_i}, w_i = \left|\sqrt{\left(x - x_i\right)^2 + \left(z - z_i\right)^2}\right|^{-2} \tag{4}$$

where y is the soil property value, x is the horizontal position, z is the vertical position, and w is the distance-based weight. Cubic spline and ordinary kriging interpolation methods were applied using the Python packages *PyKrige* (Murphy et al. 2024) and the interpolate subpackage for *SciPy* (Virtanen et al. 2020). With ordinary kriging, four variogram models were tested for all soil and root variables: linear, Gaussian, exponential, and spherical.

IDW, cubic spline, plus the four iterations of OK with different variogram models, yielded six candidate maps for each of the measured profile properties. The quality of these maps was assessed by sample variance (s^2), correlation coefficient (r), mean absolute error (MAE), and root mean squared error (RMSE) of the interpolated data compared to the sampled points. The s^2 statistics compared the feature distribution of the observed and spatially predicted target variable. The r statistic evaluated the spatial correspondence of interpolated or modeled data patterns in the maps with actual raw point observations. Finally, the error statistics (MAE and RMSE) assessed model accuracy. Using both error statistics allowed for a balance between greater penalties for the frequency of extreme values (RMSE) and equal weighting of errors (MAE) in the selection of the best-performing model.

These validation metrics were evaluated jointly in a plant-soil mapping composite score (PSMCS). The metrics were weighted equally between accuracy and pattern matching, with some additional weight given to spatial pattern matching over feature pattern matching, as shown in Eq. 5.

$$PSMCS = 0.2\left(\frac{s_i^2}{s^2}\right) + 0.3r + 0.25(MAE) + 0.25(RMSE) \quad (5)$$

where s is the variance of the sampled values and s_i is the variance of the predicted values. The respective method with the highest composite score for each soil and root property was used to generate figures using the Python package *matplotlib* (Hunter 2007). This composite score enabled consistent selection of optimal models by the weighted model fit metrics. Model quality was also evaluated with the more standard Akaike Information Criterion (AIC) and compared to assess any differences in model selection based on that statistic.

Results

2-dimensional maps of soil and root properties

We sampled maize when it was at V6 growth stage to create 2D maps at the plant scale –35 cm on either side of the row and 30 cm deep (Fig. 4). The mass of dry soil collected per composite core depth was 322 g dry soil (range: 237—397 g). The mass of dry roots collected per composite core depth was 0.17 ± 0.26 (range: < 0.01—1.87) g roots respectively. Plenty of sample for multiple soil analyses. While root mass was too small to grind and analyze for nutrients in some cases, < 0.05 g, we were still able to get mass. This was expected for maize at the V6 growth stage, and it is highly likely that greater root mass would be found later in the growing season.

Pooling all depth increments together, soil N and root properties were the most variable over this 0.2 m^2 area, with root biomass and RLD varying the most (CVs > 144%; Table 2). Soil nitrogen pools were moderately variable, with CVs between 72 and 155%. Other soil properties were much less variable at the scale of sampling, e.g., EC (23%), ρb (12.1%), and soil pH (3.7%). The 2D maps for the three individual plots, however, appeared similar for some soil and root properties, but plot nuances are apparent for others (Figures S2, S3, and S4).

The ρ_b in this zone ranged from 0.85 to 1.66 g cm^{-3} and showed evidence of lower ρ_b within 10 cm on either side of the maize row and down to 30 cm depth (Figure S2). Gravimetric soil moisture ranged from 9 to 25% and showed a clear vertical distribution with greater θ_g lower in the soil profile. Soil pH was acidic to near-neutral and ranged from 5.23 to 6.72. The soil pH reflected a pattern similar to many other properties, with the most acidic soils near the center of the row, slightly to the right, and at the surface (Figs. 4, S2). The EC ranged from 111 to 539 mS cm^{-1}, and values were greatest at 10 cm on either side of the maize, especially at the surface.

Soil N pools showed varied patterns (Figs. 4, S3). Ammonium concentrations ranged from < 1 to 48 mg N kg^{-1}, and greatest concentrations at the surface of the row, but there were also high concentrations at 20—30 cm depth in two plots. Soil nitrate concentrations ranged from < 1 to 41 mg N kg^{-1} and were concentrated on the soil surface (top 5 cm). However, some greater concentrations were lower in the profile (15—30 depth), mostly near the maize row. Salt-extractable organic N ranged from < 1 to 69 mg N kg^{-1}, and there was no uniform pattern to the pool of N in the 75 × 30 cm planes of the three plots (Figure S3). Microbial biomass N ranged from 1 to 60 mg N kg^{-1} and, like SEON, and showed no uniform distribution pattern across all three replicates (Figure S3).

The patterns in root morphology, as no surprise, occurred primarily near the crop row and at the surface (Fig. 4, S3). This is where the seed was planted. Root biomass ranged from 0 (below detection) to 1.87 g cm^{-3} and was greatest in the row and near the surface. However, roots were found out to the farthest reaches of our soil sampling. Root length density ranged from < 1 up to 355 mm cm^{-3}, and clear pattern with greater density near the row (± 20 cm) and close to the surface (< 15 cm depth). The MRD for each gridded sample ranged from 0.043 to 0.172 mm, and while two plots tended to have larger MRD at the surface or within the row, the third replicate did not (Figure S4). Some of the larger roots did seem to appear at the surface of that plot, though.

Spatial interpolation and model fitting

To determine the best-fit model for each plot, we tested three spatial interpolation approaches by using a novel composite score, PSMCS (Eq. 5). The PSMCS was largely in agreement with the AIC statistics but provided the option to emphasize different aspects of model fit for future applications. Although all interpolation methods performed well, the selection of which approach provided the optimal interpolated surface, i.e. maps, were highly variable across soil parameters and even within parameters among the replicate plots (Table 3). Furthermore, there were three incidents where the three replicated plots shared the same best-fit interpolation method, but a different best-fit method was selected for the plot means (e.g., soil pH, nitrate, MBN, and root biomass). These shifts suggest differences in locational variability may influence which method is best suited for representing patterns in the data, with plot means tending to exhibit less spatial variability.

While the three models we evaluated have some dependence on parameter settings, ordinary kriging relies on fitting a semivariogram model to the data (McBratney & Webster 1986). Depending on the soil property, the semivarigrams indicated weak to strong spatial autocorrelation. For example, the semivariance models for NH_4^+-N and root biomass

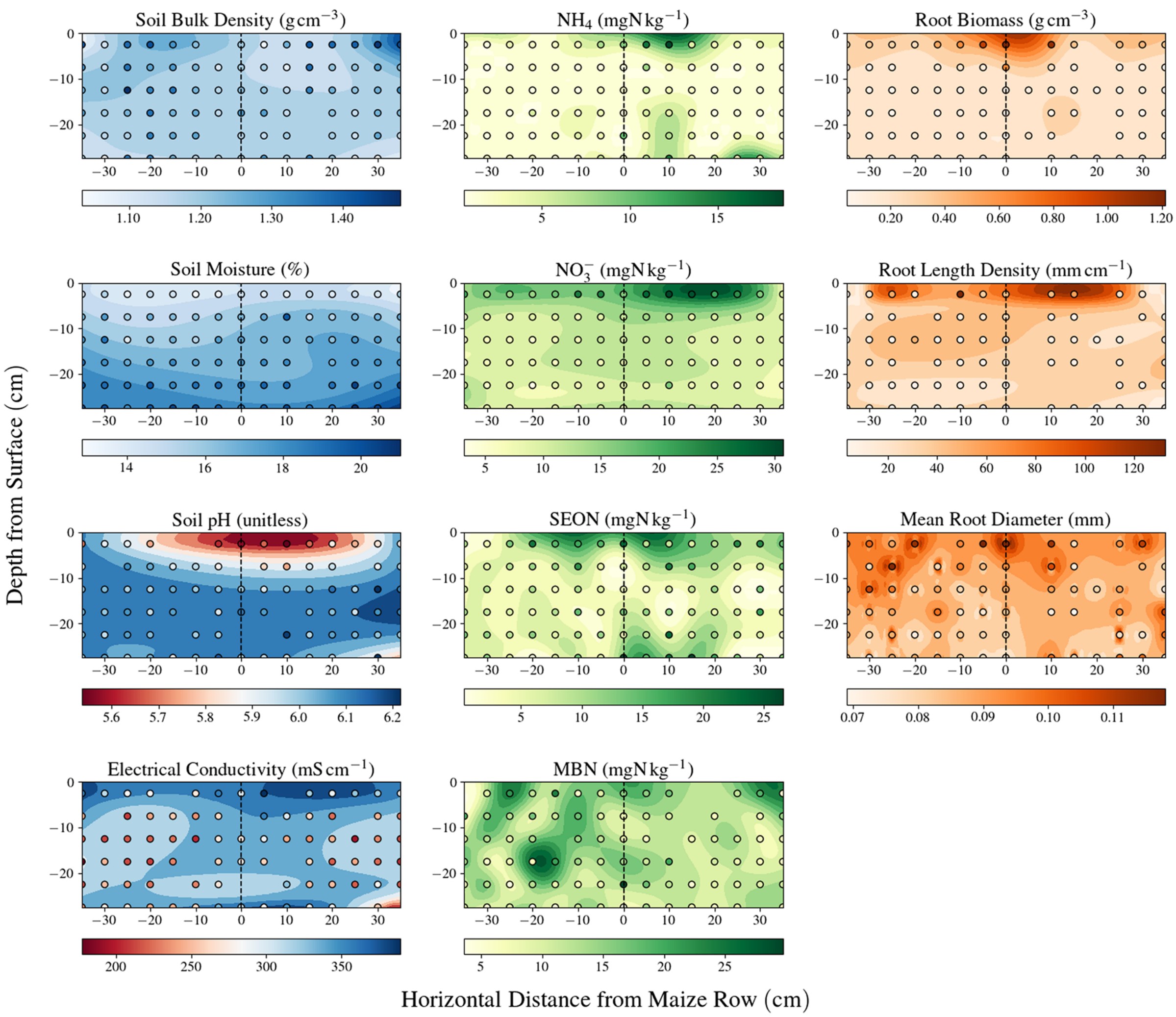

Fig. 4 Plant-scale, 2-dimensional, contour maps of soil and root properties: soil bulk density, soil moisture, soil pH, electrical conductivity, ammonium nitrogen (NH_4^+-N), nitrate nitrogen (NO_3^--N), salt-extractable organic nitrogen (SEON), microbial biomass nitrogen (MBN), root biomass, root length density, and mean root diameter. The 0 on x-axis is where the crop row is centered. Maps include interpolation with best fit mean model (Table 3); and individual dots are representing position in the grid and actual value. See Figures S2, S3, and S4 for 2D maps of the individual, replicated plots

Table 2 Descriptive statistics of soil and root properties across all three replicated plots

Soil or Root Property	Number	Mean	Standard Deviation	CV (%)	Minimum	25th Quartile	Median	75th Quartile	Maximum
Ancillary Soil Property									
Sand Content (%)	6	27.1	3.4	12.5	20.8		27.7		31
Silt Content (%)	6	37.3	4.5	12.1	32.7		36.2		45.4
Clay Content (%)	6	35.5	7.5	21.1	23.6		35.4		46.6
Primary Soil Property									
Soil bulk density (g cm^{-3})	265	1.24	0.15	12.1	0.85	1.15	1.25	1.33	1.66
Gravimetric water content (g H_2O g $soil^{-1}$)	267	17.5	2.3	13.1	8.5	16.2	17.5	19.0	25.3
Soil pH in H_2O (1:1 w:w)	258	5.97	0.22	3.7	5.23	5.81	5.99	6.12	6.72
Electrical Conductivity (mS cm^{-1})	259	261	60	23	111	220	253	295	539
Ammonium (mg N kg^{-1})	270	3.1	4.8	154.8	0.3	0.8	1.5	3.3	47.4
Nitrate (mg N kg^{-1})	269	9.6	7.0	72.9	0.4	5.3	7.6	10.7	41.0
Salt-extractable Organic Nitrogen (mg N kg^{-1})	268	11	11	100	BD	3	8	16	69
Microbial Biomass Nitrogen (mg N kg^{-1})	261	11	8	72.7	BD	6	10	14	60
Root Property									
Root Biomass (g)	258	0.18	0.26	144.4	0.01	0.05	0.09	0.16	1.87
Root Length Density (mm cm^{-3})	247	15	32	213.3	1	5	8	12	355
Mean Root Diameter (mm)	247	0.088	0.020	22.7	0.043	0.076	0.087	0.097	0.172

BD = below detection

were constant regardless of the type of model applied, while EC, θ_g, MBN, and MRD showed clear increases in semivariance with lag distance. However, even for the model semivariograms that indicated strong spatial autocorrelation, the empirical semivariogram exhibited considerable noise around those models. These results suggest that successful kriging requires large sample sets like those needed in horizontal mapping of soil properties at the landscape scale in order to have stable semivariogram models (Oliver & Webster 2014).

The majority of spatial distributions were best fit by Cubic Spline (41%) or Ordinary Kriging using a Gaussian model (45%); and the IDW model tended to be the least frequently best fitting (14%) across all data sets (Tables 3, S1, S2). Gaussian Kriging was the best fit model in at least one plot (or mean) in all variables, except for MRD. The best-fit model and map of plot mean showed very similar overall distribution to the "average" of the individual plots, illustrating that making a map of means represents the variable distribution well.

Hypothesis 1: Axis of Symmetry

Soil and root properties varied in their symmetry across the center line of the maize row (i.e., axis of symmetry; Fig. 1b). Only two variables failed all H1 tests: SEON and MBN (Table 4). All other tests at least met the null hypothesis (H_0: Slope = 1), or we had to reject that the slope is no different than a 1:1 line. Where soil and root properties began to differentiate from one another was the CCC, fit to LMM (pseudo-R^2), and the especially restrictive Wald test.

About one-half of the soil properties and 2/3 of root measurements showed some evidence of symmetry (Table 4; Fig. 5). Gravimetric water content was the most symmetrical of the soil measurements. Soil θ_g had the greatest CCC (0.767), tightest fit with LMM (pseudo-R^2 = 0.729), and only variable to pass the Walt test with 90% confidence interval within slope of 0.90 and 1.10. However, EC, pH, and NO_3^--N were also somewhat symmetrical based on the remaining two tests (CCC and pseudo-R^2). Root biomass and

Table 3 Spatial interpolation methods producing the best-fit model for the three plots individually, and for the point location means across the three plots

Soil or Root Property	Plot 1	Plot 2	Plot 3	Plot Means	Mean of 3 Plots*	Standard Deviation of 3 Plots*
Soil bulk density	Inverse Distance Weighting	Cubic Spline	Gaussian Kriging	Cubic Spline	1.25	0.03
Gravimetric water content	Inverse Distance Weighting	Gaussian Kriging	Inverse Distance Weighting	Inverse Distance Weighting	17.4	0.5
Soil pH in H_2O	Gaussian Kriging	Gaussian Kriging	Gaussian Kriging	Cubic Spline	5.96	0.18
Electrical Conductivity	Cubic Spline	Cubic Spline	Gaussian Kriging	Cubic Spline	260	9
Ammonium	Cubic Spline	Gaussian Kriging	Cubic Spline	Gaussian Kriging	3.14	1.07
Nitrate	Gaussian Kriging	Gaussian Kriging	Gaussian Kriging	Cubic Spline	9.59	1.62
Salt-extractable Organic Nitrogen	Gaussian Kriging	Cubic Spline	Cubic Spline	Gaussian Kriging	11	4
Microbial Biomass Nitrogen	Cubic Spline	Cubic Spline	Cubic Spline	Gaussian Kriging	11	1
Root Biomass	Gaussian Kriging	Gaussian Kriging	Gaussian Kriging	Gaussian Kriging	0.17	0.04
Root Length Density	Gaussian Kriging	Cubic Spline	Gaussian Kriging	Cubic Spline	14	9
Mean Root Diameter	Cubic Spline	Inverse Distance Weighting	Cubic Spline	Inverse Distance Weighting	0.09	0.01

* The descriptive statistics of the modeled populations are included to indicate the magnitude and variability of the predicted soil and root variables

RLD were similarly symmetrical (Fig. 5; Table 4), and this makes sense given the relatedness of these two root measurements. Mean root diameter, however, was not symmetrical and did not show any pattern with horizontal or vertical distribution either (Fig. 4).

Hypothesis 2: The Row Effect.

Our second hypothesis was that the management within the row – strip tillage, surface fertilizer band, seed placement (Fig. 2c) – would strongly influence soil and root properties measured when maize was at V6. Indeed, we found that these combined factors resulted in distinct soil and root properties (Fig. 6; Table S4). Although some soil and root properties were surprisingly unaffected by the row management (e.g., SEON, MBN, and MRD).

The strongest positive effects of row management across all three plots were to increase NH_4^+-N (+62%), RLD (+59%), and root biomass (+55%). The strip-tillage in the row likely contributed to a significant decrease in ρ_b, too, from 1.30 g cm^{-3} in the Control (interrow) to 1.23 in the Row (−6%). The row management also decreased soil pH from 5.96 to 5.85 (−2%), most likely due to N fertilizer placement in this zone but also somewhat by root activity.

Discussion

Novelty of sampling soil and root properties using this approach

We used an ambitious, minimally destructive sampling campaign to create accurate 2D maps of soil and root properties at the plant scale in the field (Fig. 3). Most studies pairing soil and root measurements in this way occurred in laboratory or growth chambers, or end up using trenches that destroy small-plot research. However, the mechanization of farming and precise row management that is now commonplace in agriculture make it possible to use a paired, staggered soil sampling approach in any row crop systems to test novel hypotheses. And with little disruption to the long-term research plots.

Table 4 Metrics to test Hypothesis 1: Axis of Symmetry (also see Fig. 5 and Table S3)

Soil or Root Property	Lin's Concordance Correlation Coefficient*	Nakagawa's Marginal pseudo-R^2	Slope with 90% Confidence Interval†	Null hypothesis (H_0: Slope = 1)
Soil bulk density	ns	0.066	1.549 [0.896, 2.202]	0.170
Gravimetric water content	0.767	0.729	0.976 [0.910, 1.041]	0.538
Soil pH in H_2O	0.628	0.242	1.131 [0.900, 1.136]	0.350
Electrical Conductivity	0.297	0.240	1.033 [0.790, 1.277]	0.821
Ammonium	ns	0.083	1.178 [0.659, 1.697]	0.573
Nitrate	0.432	0.295	1.842 [1.429, 2.179]	0.054
Salt-extractable Organic Nitrogen	ns	0.014	−0.049 [−0.132, 0.259]	< 0.001
Microbial Biomass Nitrogen	ns	0.034	0.391 [−0.085, 0.869]	0.036
Root Biomass	0.327	0.177	0.813 [0.563, 1.062]	0.217
Root Length Density	0.252	0.123	0.711 [0.365, 1.056]	0.168
Mean Root Diameter	ns	0.045	0.730 [0.185, 1.274]	0.415

* ns = non-significant

† Wald test: a soil or root variable is not significantly different from slope = 1 if CI is between 0.90 and 1.10

Using this approach we reconstructed a plant-scale, vertical grid of soil and root properties reflecting an individual small plot (6.86 × 6.10 m). With an n = 90, we were able to construct 76 cm wide (± 38 cm from interrow to interrow) and 30 cm deep maps of various soil and root properties (Figs. 4, S2-S4). While several studies have similarly sampled grids in an agriculture field, they have much lower sample densities compared to our 395 samples m^{-2} (Table 1), and were not co-exploring soil-root interactions at plot-scale. The earliest study we could find that sampled at this scale in row crop agriculture was Nightingale et al. (1986), where researchers sampled 51 cm on either side of the row and to 150 cm deep to make EC maps (n = 30 for a sampling density of 39 samples m^{-2}, Fig. 1).

Only two recent studies comparatively measured both root and soil properties at a similar scale and sampling densities as our study (Liu et al. 2020; Sun et al. 2023). Liu et al. (2020) sub-sampled a small portion of the soil core intended for roots to measure NH_4^+-N and NO_3^--N concentrations. Sun et al. (2023), used a pit or separate soil core to measure ρ_b and pore space, a much more disruptive approach to sampling. We used a staggered and paired sampling campaign to collect ample samples of roots and soils that could be processed in separate pathways (Figs. 3, S1), and minimize plot disturbance. This sampling design, combined with the precise fertilizer and tillage in this continuous maize system, allowed us to test two novel hypotheses (Fig. 2). But this approach could easily be applied in other row crop agroecosystems to co-map soil and root properties at the plant scale.

Future uses of mapping soil and root properties at the plant scale

Beyond introducing a novel sampling approach, we adapted spatial statistical methods commonly used for field-scale horizontal maps to produce high-fidelity vertical maps of soil and root properties. To support this plant-scale mapping, we implemented the PSMCS as an objective framework for selecting the optimal interpolation method (Tables 3, S1,

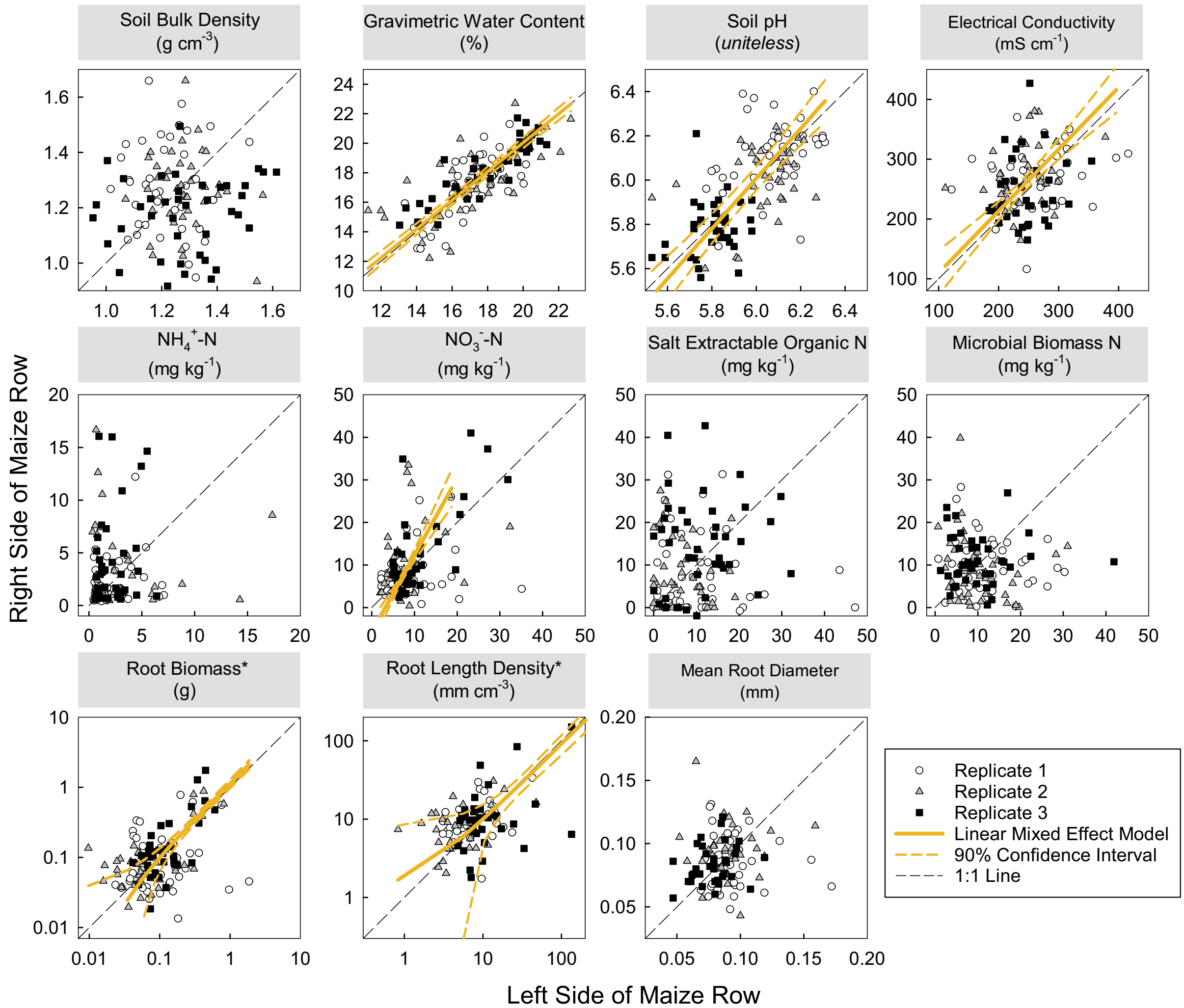

Fig. 5 Correlation between mirrored soil and root properties testing Hypothesis 1: Axis of Symmetry (Fig. 2b). On x-axis are soil properties on left side maize row, the y-axis is the same measurement paired by plot and depth. Linear mixed effect models with 90% confidence intervals shown only on variables that are significantly correlated according to Lin's Concordance Correlation Coefficient (Table 4). Asterisks (*) signify that x- and y-axes were on $\log_{10}$ scale (Root Biomass and RLD)

S2). For example, overly smooth models can mask localized hotspots, whereas overly flexible models can amplify noise and generate spurious extremes. Some interpolation models may also introduce their own method-specific patterns, which become difficult to distinguish from "true" patterns in the data. The PSMCS helps to find the best-fit, balanced model that reduces these risks. This strategy is broadly useful for spatial modelling but is especially important for soil-root profile mapping, where the sampling density is constrained by depth and degree of minimizing disturbance. Collecting and analyzing deeper soil samples is time- and labor-intensive. Not to mention becoming more disruptive to the plots. In long-term experiments, this type of sampling and mapping is best used infrequently.

Mapping spatial relationships in the soil-root environment provided insights that tables and graphs could not. These maps elucidated new patterns, clarified the context of our observations, and even pointed to possible biophysical processes contributing to them. For example, our 2D maps showed that

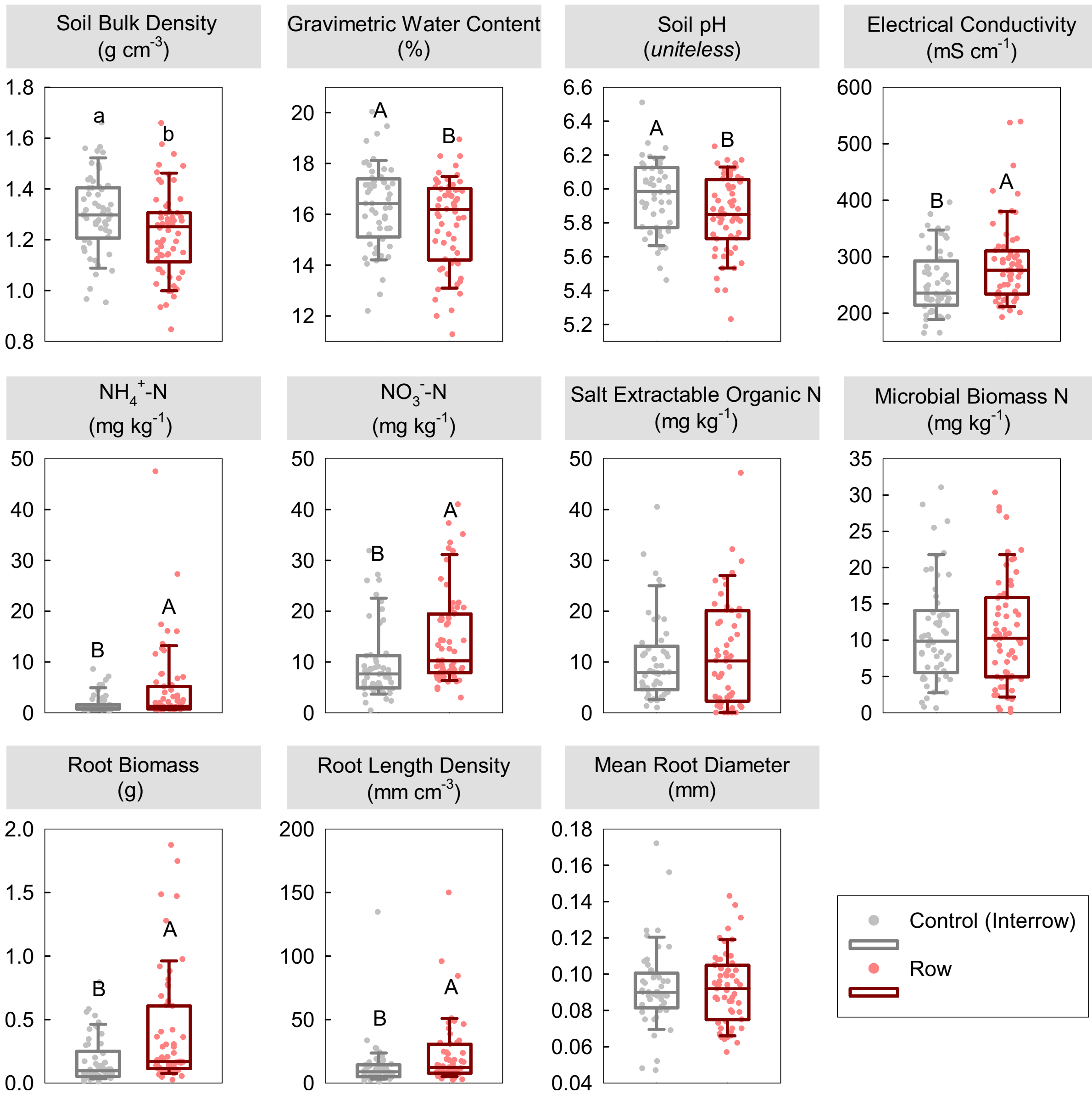

Fig. 6 Comparison between the interrow or Control zone (no-till and no fertilizer) and Row (strip-tilled, fertilizer, and majority of crop roots) to test Hypothesis 2: Row Effect (Fig. 2c). Capital letters above the boxplots indicated significant difference at $p<0.05$, lowercase letters at $p<0.1$, and letters are absent for non-significant comparisons. See Table S4 in Supplemental Materials for more details on statistics

surface soils to the right of the crop row are high in NO_3^--N, NH_4^+-N, RLD, and EC, as well as low in pH (Fig. 4). This emergent pattern was not expected with precise, center placement of fertilizer. This pattern was not reflected in simple bivariate correlation graphs (Fig. 5), but is clearly shown with individual plot maps (Figures S2-S4).

These soil and root maps also have potential management implications and can be used as guidance for correcting issues. In the soil N case mentioned above, our maps show that regardless of the precision of fertilizer management, there are “hotspots” or drift of solid fertilizer that can occur off-center from the crop row. This may be alleviated with fine-tuning of the pre-plant fertilizer equipment. Other interpretations from the maps are that strip tillage might be creating compaction walls adjacent to, and higher compaction in general, under the interrow zones (Figs. 4, S2). There are clear patterns in higher ρ_b under the interrow soil that is likely the combination of absence of tillage, and possibly greater downward force from human and machine traffic (Pöhlitz et al. 2018). Knowing where these problematic zones are allows farmers to make adjustments in order to enhance crop productivity and improve environmental quality.

Symmetry of root and soil properties (Hypothesis 1)

Sampling soil and root properties using the crop row as the axis of symmetry allowed us to also test a simple hypothesis: that soil properties to the right of the crop should be similar to those on the left (Fig. 2b). The rationale for this hypothesis is that modern, mechanized farming, with its increasingly precise tillage and fertilizer application, and the fact that root growth would be more or less random from the point of growth (i.e., seed or row center), we should observe similar values on either side of our axis of symmetry: the crop row. Indeed, we found some support for our “Axis of Symmetry” hypothesis (H1).

Six out of 11 variables showed some evidence to support H1 (Fig. 5, Table 4). The properties showing the strongest evidence of symmetry were (in decreasing order): soil θ_g, pH, NO_3^--N, RLD, root biomass, and EC. This level of symmetry extended across all three replicated plots. In the case of soil pH, we observed a clear replicate difference in pH whereby soil pH remained more-or-less symmetrical but decreased from Replicate 1 to Replicate 3. This consistent decrease in soil pH across replicates follows a toposequence up the hillslope where organic matter and calcium carbonate is expected to decrease in the gradient of soil series from Webster to Nicollet to Clarion (Soil Survey Staff 2024).

There are many reasons for the lack of symmetry in the remaining variables. The most parsimonious may be that the maize plant was only at V6 growth stage and that symmetry effect may emerge later in the growing season as the maize roots extend out further into the interrow. Other non-plant or management-related factors, however, could be causing their asymmetrical distribution (Fig. 4). For example, micro- or meso-structural differences that affect microbiota could lead to the more random distributions of SEON and MBN (Kravchenko et al. 2019; Meurer et al. 2020). Although we might expect larger roots closer to the base of the plant, the MRD did not have a clear pattern on the “left” and “right” sides of the row, nor even a strong relationship with depth (Figs. 4 and S4). Root abundance, measured as RLD and RB, were correlated strongly with NO_3^--N across the mapping space ($r_s = 0.42$ and 0.52; Figure S5). This could be due to root plasticity; and demonstrate the well-known, strong demand maize has for N at this stage in its growth (Bender et al. 2013; Mengel & Barber 1974).

While NH_4^+-N was not significantly symmetrical, most of the higher concentrations (> 4 mg N kg^{-1}) were restricted to within the width of the strip tillage equipment and surface (± 15 cm on each side of the row). However, there were some higher concentrations at lower depths, 20—30 cm (Fig. 4), that were consistently observed in all three replicates (Figure S3). This unusual pattern of NH_4^+-N distribution is puzzling. Because NH_4^+-N is positively charged, and our soils are finer textured and have quite high cation exchange capacity (CEC, Table 2), we would have expected the less mobile form of N to be mostly restricted to the top 10—15 cm (Kissel et al. 2008). Many studies show low mobility of urea-based fertilizers, especially in soils with greater CEC (Janke et al. 2022; Martinez et al. 2021; Tiessen et al. 2006). However, one study showed that given enough rainfall (150 mm), NH_4^+-N fertilizer can move > 10 cm downward into the soil profile over a 7-day period (Janke et al. 2020). This may have occurred in our soils (Figs. 4, S3). We applied fertilizer on 11 May (35 d prior to our sampling) and only received 51 mm of rainfall.

The row effect hypothesis (Hypothesis 2)

The combination of strip-tillage, surface-banded fertilizer application, and plant growth in the row was expected to exert influence over a zone 15 cm deep and ± 15 cm on either side of the maize, compared to interrow zones (Fig. 2c). This row effect hypothesis, or H2, was mostly supported in 8/11 soil and root properties. The direction of these row effects is expected to be driven either by tillage (i.e., lower ρ_b), plant growth and resource use (i.e., lower θ_g), or fertilizer application (i.e., lower pH, higher EC, greater plant-available N). Also, in the row there was 55% greater root biomass and 59% greater RLD than compared to the same depths. These findings were all expected.

It was unexpected to find no row effect on SEON, MBN, and MRD. A plethora of studies find that the rhizosphere and even the soil around the crop root have greater microbial biomass, enzyme activities, labile forms of N, and other general indicators of microbial resources and activity (Finzi et al. 2015). One explanation for the lack of an effect on MBN and SEON is that fertilizer and strip-tillage may have counteracting negative effects on the positive "root effect" in the center row. Indeed, there is substantial evidence of adverse effects of tillage on microbial biomass (Zuber & Villamil 2016), which may also extend to SEON because where there is lower microbial biomass there is less N turnover, and perhaps less residual low-molecular weight organic N. Some evidence shows that no-tillage can increase extractable forms of organic N, like SEON (Sharifi et al. 2008; R. Sun et al. 2015). Alternatively, maize was somewhat early in its development and that positive rhizosphere effects on microbial biomass, at least at this scale, might have emerged later in the growing season if we had sampled then.

Conclusion

A clearer understanding of soil-root interactions that govern agroecosystem processes enables management decisions that can improve the sustainability of modern, mechanized agriculture. Visualizing where these interactions occur is key. Here, we demonstrated a minimally destructive approach to create 2D maps of both soil and root properties at the plant scale (76 × 30 cm), each representing individual small research plots. Furthermore, we used this approach to test two hypotheses. We hypothesized that soil and root properties would be symmetrical on either side of the maize row and found some evidence to support this. Second, we hypothesized that strip tillage, fertilizer band, and growth point would strongly influence soil and root properties. Such was the case for 8/11 of our measurements. Those measures for which we did not see a difference between the row soil and the surrounding interrow soil may reflect countervailing management effects on soil microbes and biological activities (e.g., positive effects of crop roots but negative effects of tillage). This strategic, paired approach to create plot-level, 2D maps of soils and roots can be used to compare management practices at a finer scale than traditional experimental designs, improving our understanding of soil–plant interactions under row crop agriculture.

Acknowledgements This work was funded by the USDA-NIFA SAS (Grant #2021-68012-35923). We want to thank collaborator Dr. Shuizhang Fei for the foresight to establish the long-term experiment, and Mr. Roger Hintz for expert precision management of the agronomy in this experiment. We would like to thank the many folks in the McDaniel, Moore, and VanLoocke Labs who helped with soil sampling and processing. Finally, we extend much gratitude to Dr. Michael Thompson for providing critical feedback on early draft of this manuscript.

Data availability Data generated in this manuscript will be available upon reasonable request from the corresponding author. It will also be available at Iowa State University digital repository (https://doi.org/10.25380/iastate.32288322).

References

Bates D, Mächler M, Bolker B, Walker S (2014) Fitting linear mixed-effects models using lme4. ArXiv Preprint ArXiv:1406.5823

Bender RR, Haegele JW, Ruffo ML, Below FE (2013) Nutrient uptake, partitioning, and remobilization in modern, transgenic insect-protected maize hybrids. Agron J 105(1):161–170

Blackmer AM, Pottker D, Cerrato ME, Webb J (1989) Correlations between soil nitrate concentrations in late spring and corn yields in Iowa. J Prod Agric 2(2):103–109

Böhm W (2012) Methods of studying root systems (Vol. 33). Springer Science & Business Media

Brookes PC, Landman A, Pruden G, Jenkinson DS (1985) Chloroform fumigation and the release of soil nitrogen: a rapid direct extraction method to measure microbial biomass nitrogen in soil. Soil Biol Biochem 17(6):837–842. https://doi.org/10.1016/0038-0717(85)90144-0

Dietzel R, Liebman M, Archontoulis S (2017) A deeper look at the relationship between root carbon pools and the vertical distribution of the soil carbon pool. Soil 3(3):139

Doane TA, Horwáth WR (2003) Spectrophotometric determination of nitrate with a single reagent. Anal Lett 36(12):2713–2722. https://doi.org/10.1081/AL-120024647

Dutter CR, Rutkoski CE, Evans SE, McDaniel MD (2024) Contour prairie strips alter microbial communities and functioning both below and in adjacent cropland soils. Appl Soil Ecol 199:105424

Finzi AC, Abramoff RZ, Spiller KS, Brzostek ER, Darby BA, Kramer MA, Phillips RP (2015) Rhizosphere processes are quantitatively important components of terrestrial carbon and nutrient cycles. Glob Chang Biol 21(5):2082–2094

Freschet GT, Pagès L, Iversen CM, Comas LH, Rewald B, Roumet C, Klimešová J, Zadworny M, Poorter H, Postma JA (2021a) A starting guide to root ecology: strengthening ecological concepts and standardising root classification, sampling, processing and trait measurements. New Phytol 232(3):973–1122

Freschet GT, Roumet C, Comas LH, Weemstra M, Bengough AG, Rewald B, Bardgett RD, De Deyn GB, Johnson D, Klimešová J (2021b) Root traits as drivers of plant and ecosystem functioning: current understanding, pitfalls and future research needs. New Phytol 232(3):1123–1158

Gao J, Zhang F, Zhang J, Zhou H, Yuan T (2023) Development and field performance evaluation of hole-fertilizing planter and dynamic alignment control system for precision planting of corn. Precis Agric 24(4):1241–1260

Gomes NCM, Fagbola O, Costa R, Rumjanek NG, Buchner A, Mendona-Hagler L, Smalla K (2003) Dynamics of fungal communities in bulk and maize rhizosphere soil in the Tropics. Appl Environ Microbiol 69(7):3758–3766. https://doi.org/10.1128/AEM.69.7.3758-3766.2003

Goode K, and Rey K (2019) ggResidpanel: panels and interactive versions of diagnostic plots using 'ggplot2.' R Package Version 0.3. 0. Online< https://Cran.r-Project.Org/Web/Packages/GgResidpanel/Index.html

Hunter JD (2007) Matplotlib: a 2D graphics environment. Comput Sci Eng 9(03):90–95

Janke CK, Moody P, Bell MJ (2020) Three-dimensional dynamics of nitrogen from banded enhanced efficiency fertilizers. Nutr Cycl Agroecosyst 118:227–247

Janke C, Moody P, Fujinuma R, Bell M (2022) The impact of banding polymer-coated urea on nitrogen availability and distribution in contrasting soils. J Soil Sci Plant Nutr 22(3):3081–3095

Kissel DE, Cabrera ML, Paramasivam S (2008) Ammonium, ammonia, and urea reactions in soils. Nitrogen in Agricultural Systems 49:101–155

Kravchenko AN, Guber AK, Razavi BS, Koestel J, Quigley MY, Robertson GP, Kuzyakov Y (2019) Microbial spatial footprint as a driver of soil carbon stabilization. Nat Commun 10(1):1–10

Lawrence I, Lin K (1989) A concordance correlation coefficient to evaluate reproducibility. Biometrics. https://doi.org/10.2307/2532051

Liu Y-X, Sun J-H, Zhang F-F, Li L (2020) The plasticity of root distribution and nitrogen uptake contributes to recovery of maize growth at late growth stages in wheat/maize intercropping. Plant Soil 447:39–53

Martinez C, Clarke D, Dang YP, Janke C, Bell MJ (2021) Integrated field assessment of nitrogen release dynamics and crop recovery of band-applied controlled-release fertilisers. Plant Soil 466(1):257–273

McBratney AB, Webster R (1986) Choosing functions for semi-variograms of soil properties and fitting them to sampling estimates. J Soil Sci 37(4):617–639

Mengel DB, Barber SA (1974) Development and distribution of the corn root system under field conditions 1. Agron J 66(3):341–344

Mesonet I (2024) ISU Mesonet - Iowa State University Iowa Environmental Mesonet Climate Data. https://mesonet.agron.iastate.edu/

Meurer K, Barron J, Chenu C, Coucheney E, Fielding M, Hallett P, Herrmann AM, Keller T, Koestel J, Larsbo M (2020) A framework for modelling soil structure dynamics induced by biological activity. Glob Change Biol 26(10):5382–5403

Murphy B, Yurchak R, Müller S (2024) GeoStat-Framework/PyKrige: v1.7.2 (v1.7.2). In Zenodo

Nakagawa S, Schielzeth H (2013) A general and simple method for obtaining R2 from generalized linear mixed-effects models. Methods Ecol Evol 4(2):133–142

Nardon GF, Botta GF (2022) Prospective study of the technology for evaluating and measuring in-row seed spacing for precision planting: a review. Span J Agric Res 20(4):e02R01-e02R01

Nightingale HI, Davis KR, Phene CJ (1986) Trickle irrigation of cotton: effect on soil chemical properties. Agric Water Manag 11(2):159–168

Oliver MA, Webster R (2014) A tutorial guide to geostatistics: computing and modelling variograms and kriging. CATENA 113:56–69

Pöhlitz J, Rücknagel J, Koblenz B, Schlüter S, Vogel H-J, Christen O (2018) Computed tomography and soil physical measurements of compaction behaviour under strip tillage, mulch tillage and no tillage. Soil Tillage Res 175:205–216

R Core Team (2023) R: A language and environment for statistical computing. R Foundation for Statistical Computing. <https://www.R-project.org/>

Seethepalli A, Guo H, Liu X, Griffiths M, Almtarfi H, Li Z, Liu S, Zare A, Fritschi FB, Blancaflor EB (2020) Rhizovision crown: an integrated hardware and software platform for root crown phenotyping. Plant Phenomics. https://doi.org/10.34133/2020/3074916

Sharifi M, Zebarth BJ, Burton DL, Grant CA, Bittman S, Drury CF, McConkey BG, Ziadi N (2008) Response of potentially mineralizable soil nitrogen and indices of nitrogen availability to tillage system. Soil Sci Soc Am J 72(4):1124–1131

Sinsabaugh RL, Reynolds H, Long TM (2000) Rapid assay for amidohydrolase (urease) activity in environmental samples. Soil Biol Biochem 32(14):2095–2097. https://doi.org/10.1016/S0038-0717(00)00102-4

Soil Survey Staff (2024) Web soil survey: natural resources conservation service, united states department of agriculture. Elsevier. https://websoilsurvey.nrcs.usda.gov/app/

Sun R, Zhang X-X, Guo X, Wang D, Chu H (2015) Bacterial diversity in soils subjected to long-term chemical fertilization can be more stably maintained with the addition of livestock manure than wheat straw. Soil Biol Biochem 88:9–18

Sun Q, Sun W, Zhao Z, Jiang W, Zhang P, Sun X, Xue Q (2023) Soil compaction and maize root distribution under subsoiling tillage in a wheat-maize double cropping system. Agronomy Basel 13(2):394

Taylor HM (1986) Methods of studying root systems in the field. HortScience 21(4):952–956

Tiessen KHD, Flaten DN, Bullock PR, Burton DL, Grant CA, Karamanos RE (2006) Transformation of fall-banded urea: application date, landscape position, and fertilizer additive effects. Agron J 98(6):1460–1470

Vance ED, Brookes PC, Jenkinson DS (1987) An extraction method for measuring soil microbial biomass C. Soil Biol Biochem 19(6):703–707

Virtanen P, Gommers R, Oliphant TE, Haberland M, Reddy T, Cournapeau D, Burovski E, Peterson P, Weckesser W, Bright J (2020) SciPy 1.0: fundamental algorithms for scientific computing in Python. Nat Methods 17(3):261–272

Wang Q, Wang B, Sun M, Sun X, Zhou W, Tang H, Wang J (2023) Design and testing of an automatic strip-till machine for conservation tillage of corn. Agronomy Basel 13(9):2357

Wasson AP, Nagel KA, Tracy S, Watt M (2020) Beyond digging: noninvasive root and rhizosphere phenotyping. Trends Plant Sci 25(1):119–120

Wollum AG (1994) Soil sampling for microbiological analysis. Methods of Soil Analysis: Part 2 Microbiological and Biochemical Properties 5 1–14

Zuber SM, Villamil MB (2016) Meta-analysis approach to assess effect of tillage on microbial biomass and enzyme activities. Soil Biol Biochem 97:176–187